Investigation of Surface Treatment of Carbon Fiber by Dynamic Method in the Polyurethane Composites

Mohamad Reza Pourhossainy ⓘ**, Amir Kaveh** * ⓘ **, Morteza Ahmadi Lashaki** ⓘ**, Mahdi Jafari** ⓘ**, Omid Moini Jazani** ⓘ

1. Faculty of Materials and Manufacturing Engineering, Malek Ashtar University of Technology, Tehran, Iran. E-mail: mrp_polycrc@mut.ac.ir
2. Department of Polymer Engineering, Amirkabir University of Technology, Tehran, Iran. E-mail: p90132910@aut.ac.ir
3. Department of Chemical Engineering, Iran University of Science & Technology, Tehran, Iran. E-mail: ahmadi.morteza@yahoo.com
4. Department of Aerospace engineering, Malek Ashtar University of Technology, Tehran, Iran. E-mail: m.jafari.h@mut.ac.ir
5. Department of Chemical Engineering, Faculty of Engineering, University of Isfahan, Isfahan, Iran. E-mail: o.moini@eng.ui.ac.ir

ARTICLE INFO	ABSTRACT
	Polyacrylonitrile (PAN)-based carbon fibers were chemically modified with a different ratio of Sulfuric acid (SA) to Nitric acid (NA), then reinforced Polyurethane (PU) composites in the presence of carbon fibers were prepared. The structural and surface characteristics of the modified carbon fibers were investigated by scanning electron microscopy (SEM), Fourier transforms infrared spectroscopy (FTIR), and X-ray diffraction (XRD). The FTIR results showed the presence of the carbonyl groups in a higher ratio of NA and the formation of carboxyl groups in a lower ratio of NA. The interaction between carbon fiber and PU matrix was studied by the dynamic mechanical thermal analysis (DMTA) method. The DMTA results showed with increasing carbon fiber/PU matrix interaction, the intensity of glass transition temperature decreased. Matching the DMTA results with the power-law model and Cole-Cole diagram showed that the process of carbon fiber modification can increase the amount of chain with a long relaxation time in the PU matrix.

Introduction

Dispersing and orientation of the short or long fibers in polymeric materials provide a scientific and industrial interest in polymer composites. The interface of the matrix and reinforcement fibers as a key factor can be an advantage or a drawback in the filled materials. A proper and compatible junction can improve some dynamic and mechanical properties, and organosilane-based coupling agents were mentioned as a fruitful smoother of this path [1]. Proper interaction of Polyurethane (PU) elastomers and carbon fibers (CF) is a reason to omit this relatively expensive coupling agent, the organosilane [2, 3]. Then, PU composites have a particular situation in a variety of use such as buildings and construction, aerospace, electronics,

---

and so on [4-6]. Low viscosity and then facile processability, high resistivity against abrasion, low price, and short reaction time are other advantages of this elastomer. The most prevalent one-dimensional reinforcers for the polymeric matrix are glass and carbon fibers.

Due to the remarkable elasticity of PU and the high stiffness of carbon fiber, their composite is worthy of attention too much [7]. Short or long carbon fibers can be entered into the matrix via a fast molding process [8]. However, random orientation and/or fiber fracture during the molding process causes a downfall in final product properties than full-oriented fibers aligned in the matrix. Usually, non-treated carbon fibers have a powerless bond with the polymeric matrix as a consequence of their inborn smoothness and chemical neutrality [3]. Copious attempts have been done to treat the surface of carbon fiber for better adherence of fiber surface to polymeric matrix [9-11]. Removing the destroyed layer of fiber and increasing the number of surface-active groups are two steps of surface treatment. Oxidation, chemical scratching, plasma scratching [12], chemical vapor sedimentation [13, 14], gamma-ray radiation [15, 16], and ionic induction [17] are different types of surface treatment methods.

During chemical treatment, functional groups are produced on the surface of carbon fibers. The concentration of the oxidizing agent, time, temperature, and fiber nature is the most effective parameters which affect chemical treatment quality. Usually, oxidation is done through gases (air, oxygen, and ozone) or liquids (NA, Sulfuric acid, hydrochloric acid, etc.). Sellitti et al. [18] carried out the oxidation of Rayon-based graphitized CF for 5, 15, and 25 hrs, and the presence of carboxylic acid, ester, lactone, enol, and quinone structure studied by Fourier transform infrared attenuated total reflection spectroscopy (FTIR-ATR) spectra. Feng et al. [19] reinforced Epoxy(EP) composites with PEI-functionalized CFF, which were prepared by grafting with PEI after pre-deposition of PDA on the CF surface and were fabricated and investigated their mechanical and thermal properties. The results showed notable improvements in flexural strength, flexural modulus, and ILSS) and thermal) properties. He investigated the reinforcing mechanism by SEM, DMA, and DSC and indicates the PEI-functionalization of CF increases the crosslinking density of interphase between PEI-PCFF and EP matrix. Tran et al. [20] showed by modification of CFs by boiling for 5h in HNO3, the surface oxygen and nitrogen content increased and led to a rise in fiber overall surface energy. Rand and Robinson [21] carried out the oxidation of CFs by refluxing with 68% fuming NA for periods of 9, 12, 25, and 50 hours and the increment in the external surface area of the fibers by a factor of 3.7 after 50 hours treatment in the form of edge, or active sites observed. Jang and Yang [22] used the refluxing CFs in 60% NA for 40, 60, and 80 min at 100 0C for oxidation of CF fiber and observed that the (Brunauer-Emmett-Teller) BET surface area of 60 min treated CF is 10 times larger than the untreated CF. He found that the O1s/C1s ratio increased with the acid treatment time. Zhang et al. [23] applied the strong HNO3 for the oxidation of PAN-based CFs by heating (90°C) for 1.5 h. They observed that the CF surface became rougher and the oxygen concentration increased greatly after surface treatment that this subject can improve the adhesion between the fiber and the PI matrix. The results showed the treatment created more active groups (–O–C–, –C=O, –O–C=O) on the CF surface, which increased the total surface energy, polarity, and wettability of the CFs with the matrix.

Li [24] oxidation of CFs carried out by NA treatments improves interfacial adhesion with polyimide matrix. The XPS analysis showed that the oxidation not only affects the oxygen concentration but also created a change in the chemical functions as the conversion of hydroxyl-type oxygen into carboxyl functions. Zhang et al. [25] the oxidation of pitch based CF, performed by heating CFs in NA (65–68%wt) at 90°C for 1.5 h and observed after the treatment process the active sites for van der Waals and hydrogen bonding on the CF surface increased and this subject improved the interfacial adhesion between the fibers and the surrounding PI matrix. Su et al. [26] performed the modification of carbon fabric by strong HNO3 etching by

immersing in a 13 mol/L HNO3 solution for 2 hrs. He observed the active groups created during the oxidation process, which related to strengthening the bonding strength between the fabric and the matrix. XPS results showed a little decrease in the C concentration and a minor increase in the O concentration on fabric. At the same time, the N concentration of the fabric significantly decreased by etching with HNO3. Tiwari et al. [27] treated CF by boiling in NA (HNO3, 65-68%) at 110 °C. The acid treatment was performed for a period of 15 to 180 minutes and found with increasing treatment time the roughness of the fiber surface increased and in the treated CF the ether, carboxyl, and carbonyl groups indicated peaks at the range of 950-1200 cm-1 and 1650-1710 cm-1 respectively. The presence of these groups increased its chemical reactivity and wettability with the matrix. The results showed with an increase in treatment time pick up of matrix by fabric increased sharply up to 60 minutes, followed by a slow rise to 90 minutes.

Florek et al. [41] attempted to improve adhesion between carbon fiber and epoxy resin in their research. For this purpose, graphene oxide nanoparticles were dispersed in a polymer matrix. The results of the three-point bend test showed that the strength of made samples with added graphene oxide increased. Hwang et al. [42] investigated Dual-sizing effects with either epoxy or Polyurethane (PU) on the thermal, and mechanical properties of carbon fiber/acrylonitrile-butadiene-styrene (ABS) composites produced by extrusion and injection molding processes. His results showed that the dual-sized carbon fiber significantly contributed not only can improve the heat deflection temperature and the storage modulus, but also can improve the tensile, flexural, and impact properties of carbon fiber/ABS composites. Zhao et al. [43] manufactured carbon fiber (CF) plain-woven fabric-reinforced polyamide 6 (PA6) laminates by the hot-compression technique. Then, the carbon plain-woven was modified with Polyurethane dispersion (PUD) to improve the compatibility and interaction increasing with PA6. His results of flexural tests and low-cycle flexural fatigue tests demonstrated that compared with a composite without PUD treatment, treated CF/PA6 laminates not only exhibit enhancement in flexural strength but also acquire improvement in residual flexural strength retention after fatigue tests.

In this paper, the effect of acidic chemical treatment with the different volume ratios on the surface properties of carbon fiber was investigated and the interaction between modified carbon fiber and Polyurethane matrix was studied with the DMTA method.

Experimental

Carbon fibers used in these experiments were provided by the Toray Company. Nitric acid (NA, 65%), Sulfuric acid, (SA, 95%), Toluene diisocyanate (TDI), toluene, and dibutyltin dilaurate (DBTDL, catalyst), all were purchased from the Merck chemical company. Polypropylene Glycol (PPG, MW = 2000 g/mol, OH value = 54.94 mg KOH/g) and trimethylolpropane (TMP, crosslink agent) were procured from the Aldrich chemical company. For desizing the purchased carbon fiber, they were put in boiled distilled water for one hour, and then they were kept in a vacuum oven at 80 °C for about 2 hours to be dried. Treatment operation was done with different ratios of NA to SA. Table 1, shows the amount of CF, NA, and SA in a balloon (250 cc) including three entrances. Samples were stirred under ultrasonic waves for four minutes and then were treated at 85 °C with a reflux system. For neutralizing the reaction atmosphere, nitrogen gas was used. Then, mixtures were filtered and for washing to remove the remainder acid, distilled water was applied. Then samples were kept in a vacuum oven at 60 °C for about 10 days to fulfill drying. TDI was enchased on treated carbon fiber by mixing 2g CF, 2 cc TDI, 100 cc toluene and 2 drops DBTDL inside a balloon for about 3 hr with a reflux system and at 80 °C under N_2. Samples were filtered and washed with toluene. Sized fibers were dried under vacuum and at 60 °C for about 10 hrs.

Table 1. Composition of acid treatment processes of fibers

NA: SA (volume ratio)	Carbon fiber (g)	NA (cm³)	SA (cm³)
2:1	2	60	30
1:1	2	45	45
1:2	2	30	60

PPG, TMP, and TDI were mixed (NCO/OH ratio =1.2) and reacted by the equivalent ratio of NCO group to total OH group equal to 1.2. The weight of the curing agent was determined according to Eq. 1:

$$\text{Wt. of TDI} = 1.2 \times \text{Eq. wt. of TDI} \times \left[\frac{Wt.\,of\,PPG}{\text{Eq. wt. of PPG}} + \frac{Wt.\,of\,TMP}{\text{Eq. wt. of TMP}}\right] \quad (1)$$

The equivalent weight of PPG was determined according to Eq. 2:

$$\text{Eq. wt. of PPG} = \frac{56100}{OH\,no} \quad (2)$$

In the beginning, 10g PPG was transferred to a balloon and then TMP ($OH_{triol}/OH_{total}=0.39$) was added. These alcohols were stirred for 30 min. at 70 ℃ under a vacuum to omit the moisture. By cooling them to ambient temperature, TDI was injected into the system by a syringe, and the balloon was degassed. By ending bubbling, the catalyst, DBTDL ($\frac{\text{mol DBTDL}}{\text{mol polyol}} = 0.05$) was added. Treated carbon fibers (5 wt%) were aligned axially in the silicone mold (30mm×9mm×3mm) and PU, far before its gel point was added. Then, the autoclave was used during curing at 60℃ under a vacuum to have void-free samples. A Thermo-Nicolet FTIR-ATR (model Nexus 670) was used for spectroscopy of the fibers' surfaces. An X-ray diffractometer (XRD), made in Intel, France, model Equinox 3000 (I= 40 mA, V= 450 Kv, λ=0.15418 nm) was used to characterize fibers. Tensile properties of treated and sized monofilaments were measured by Instron, model 56565, according to ASTM 3379. A scanning electron microscope (SEM), model JXA-840, made in Japan, Jeol company was applied to observe the surface of treated fibers. A dynamic-mechanical thermal analyzer (DMTA), model 800 Perrking was used for the investigation of the dynamic mechanical properties of composites. According to ASTM D7028-07, samples were prepared someway the dimensions were 2mm, 10mm, and 40mm. Measurements were done at a temperature range of -80 to 100 ℃, frequency of 1 Hz, and heating rate of 5 ℃ /min.

Results and Discussion

As shown in Fig. 1 non-oxidized surface of carbon fiber includes the –CH group. After oxidation of fiber surface and by progressing oxidation, -OH group is produced and then changes to a carbonyl group. More oxidation causes the creation of the carboxyl group [28]. Finally, one step more oxidation proceeding is the reason for the chemical degradation of the carboxyl group and then CO_2 formation. In this stage, characteristic peaks on the surface of carbon fiber are removed.
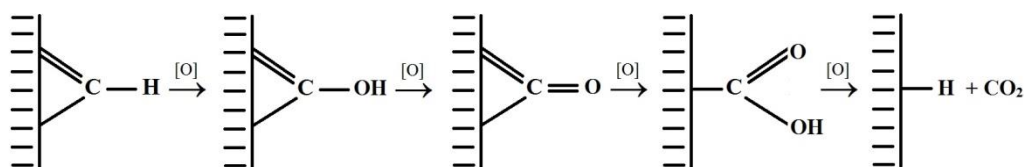
Fig. 1. Molecular representation of gradual oxidation process of carbon fiber surface [28]
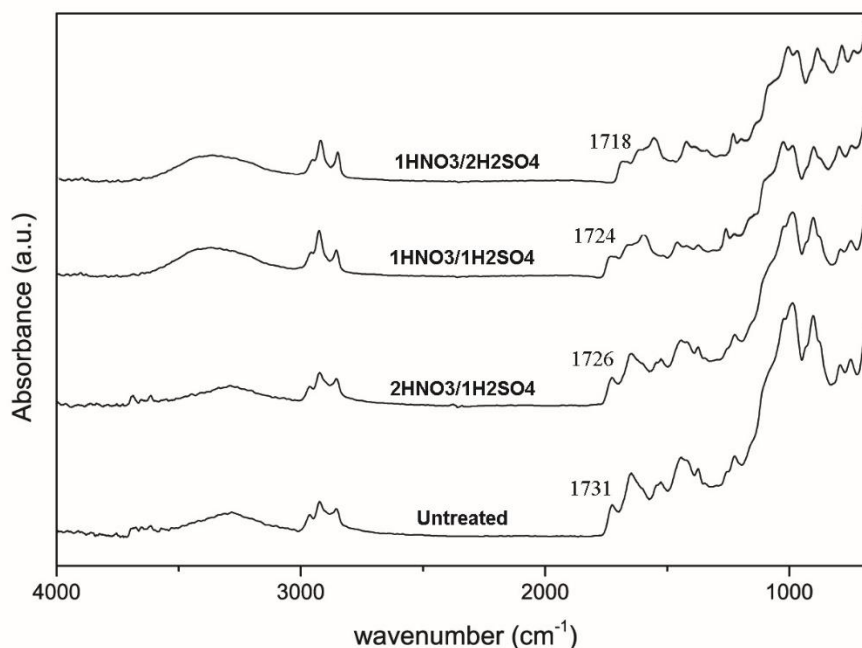

Fig. 2. FTIR-ATR spectroscopy of untreated and treated fibers

Fig. 2 shows the FTIR-ATR spectroscopy of untreated and treated carbon fiber. Observed peaks in the range of 1550-1650 cm^{-1} are related to the stretching of bonds C=C and C-N probably overlapped with the non-symmetric stretching vibration of carboxyl groups. Monitored peaks in the range of 1700-1730 cm^{-1} are related to the stretching vibration of carbonyl and carboxyl groups. Peaks in the range of 2800-3000 cm^{-1} are due to the stretching motion of C-H groups, and a wide peak in the range of 3200-3700 cm^{-1} is because of the stretching vibration of OH groups. By detecting the absorbance in the range of wave numbers 1700 cm^{-1} to 1730 cm^{-1}, conversion of carbonyl to carboxyl group can be detected. Sitting hydroxyl groups that are electrophile beside carboxyl groups causes taking an electron from carboxyl groups and reduces the wave numbers related to these latter groups. As can be seen in Fig. 2, by increasing the SA content of the NA-SA mixture in oxidized samples, the wavenumber associated with the carbonyl group decreased in this way: 1731, 1726, 1724, and 1718 for samples, untreated and treated with the NA to SA ratios 2:1, 1:1 and 1:2, respectively. Decreasing the wavenumber by increasing SA content is related to the alteration of carbonyl to the carboxyl group.

Fig. 3 shows the mechanism of acidic surface treatment and sizing of carbon fiber by TDI [11]. One NCO group reacts with one OH or COOH group that produces NHCOO or NHCOCOO groups. Then, the wavenumber of the carboxylic group in the FTIR-ATR spectra decreases due to new electrophile groups connected to C=O instead of the last OH group. Wavenumber reaches 1640 cm^{-1}, which confirms the chemical reaction of treated fiber and TDI.
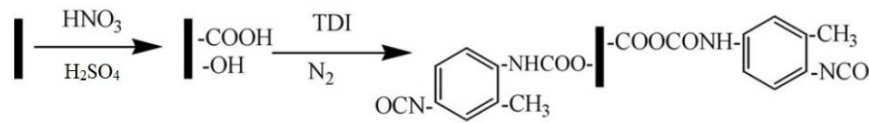
Fig. 3. Mechanism of acidic surface treatment and sizing of carbon fiber by TDI [11]

Wavenumber 2273 is related to the NCO group that is a basis for the comparison of sizing efficiency. Fig. 4 compares FTIR-ATR spectroscopy of treated and sized fibers. It shows by increasing SA content in NA-SA mixture, absorbance intensity of NCO group raises too, the criterion of more efficient sizing. An intense peak at wave number 3430 cm^{-1} can also be seen related to groups NH and OH due to the connection of TDI to the fiber surface.
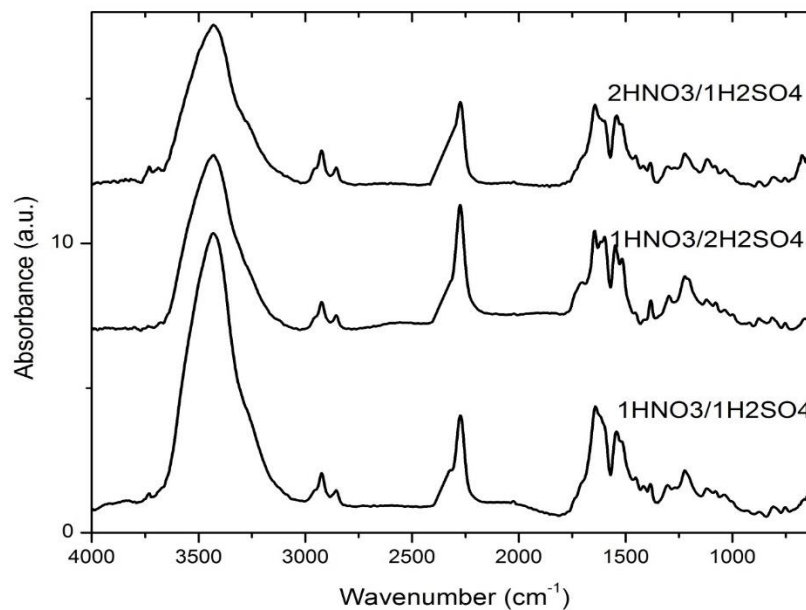

Fig. 4. FTIR-ATR spectroscopy of treated and sized fibers

Fig. 5 compares the XRD patterns of untreated and different treated carbon fibers. Semi-graphitic plates in carbon fibers can be detected by peaks 002, and their distance can be determined. For the ideal graphite, the distance of 0.335 nm was reported [29]. Of course, in the semi-graphitic plates of carbon fiber, the distance is more than ideal graphite. According to Fig. 5, for untreated fiber, the peak 002 exists at $2\theta = 25.5°$ and by the Bragg equation, the distance is about 0.35nm [30, 31]. Surface treatment can increase the distance due to the presence of functional groups. According to Fig. 5, the distance has not been changed when the treatment was done by the SA-NA mixture by the ratio NA: SA equal to 2:1 and the FTIR-ATR spectrum verifies it. By increasing the oxidation power, a bigger interlude was created. A combination of results obtained from XRD and FTIR-ATR shows that more oxidation power or more SA in the acidic mixture causes a bigger inter-plate distance ex parte, and from the other side, it goes far away from the ideal graphitic structure and also the presence of some defects in it that reduces the mechanical properties of the fiber. On the other hand, more functionality of CF surfaces is due to more oxidation power that improves the interaction between fiber and matrix, and then mechanical properties of composite will enhance.
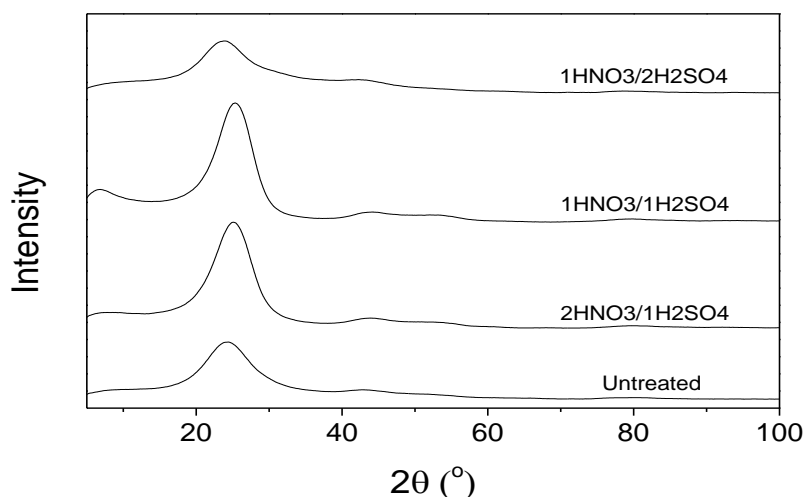
Fig. 5. XRD pattern of untreated and treated CFs

By calculating the distances between graphitic platelets, the Scherrer equation can determine the thickness of a clump of plates stuck together. According to Table 2, chemical oxidation reduces crystals' dimensions. However, by surface oxidation, the distance between crystal platelets increases, but because of crystal breaking, the mechanical properties of CF reduce. The results in Table 2 do not show a clear trend for this competition in the race. Then, it is necessary to measure the mechanical properties to find the direct effect of variation in oxidation on the properties of CFs.

Table 2. XRD results of untreated and treated CF

NA: SA (volume ratio)	$2 \theta(^{o})$	d [Å] Interlayer distance	Lc [Å] Size of crystallite
untreated	25.52	3.5	19.22
2:01	25.25	3.5	12.44
1:01	23.79	3.6	18.11
1:02	24.48	3.7	14.88

Fig. 6 shows scanning electron micrographs (SEM) of untreated (a) and treated CFs by the NA to SA ratios 2:1 (b), 1:1 (c), and 1:2 (d). Untreated fibers show smooth surfaces without any pores or defects on them, but the surface treatment caused a coarseness and is enhanced by increasing the power of oxidation. The creation of these defects results in strength reducing of fibers from one side and producing a hand to take the hand of the matrix from another side. These physical junctions can help the chemical connections resulting in functional groups to improve the mechanical properties of composites.
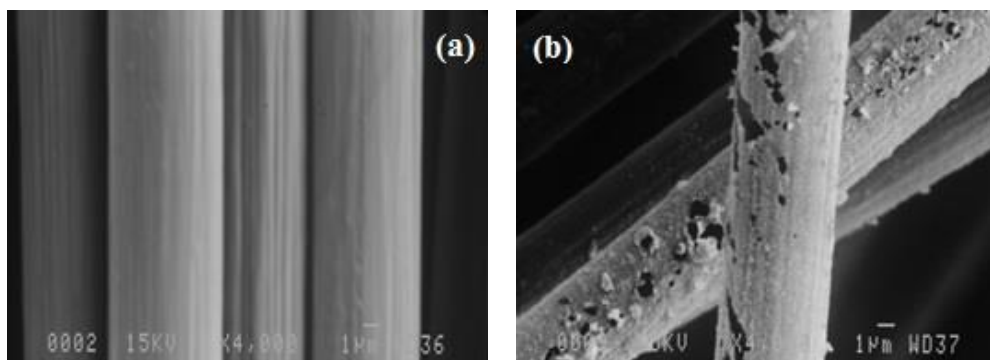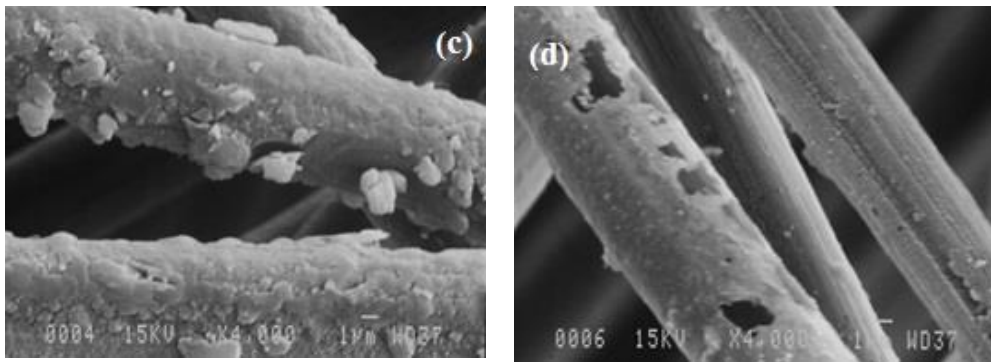
Fig. 6. Scanning electron micrographs of untreated (a) and treated CFs by the NA to SA ratios 2:1 (b), 1:1 (c), and 1:2 (d)

Variations of storage modulus as a function of temperature are shown in Fig. 7. Temperature elevating decreased the storage modulus of all samples. The reason is the motion freedom of polymer chains [32]. It can be seen that adding fibers to PU causes raising the storage modulus in the rubbery regions. This elevating that is seen even in the presence of untreated fibers is due to the attendance of very high stiff fibers. Nevertheless, it is expected that by increasing the interactions and decreasing the freedom of chain motions storage modulus increases [33]. Fig. 7 shows the storage modulus of PU-CF composites as a function of temperature and surface treatment of fibers for sized fibers. According to Fig. 7, Oxidative surface treatment followed by reaction with isocyanate, TDI, increases the storage modulus in the rubbery region and then fortifies the CF-PU interface. A higher ratio of SA to NA causes more increase in the modulus due to progressing oxidation and producing carboxylic groups, and also etching of the surface of CF. More SA in the acidic mixture demolishes the surface of fibers.

Whereas, in sample 2:1, the increase of SA content doesn't change the value of the storage modulus. This phenomenon is related to the more degradation of carbon fiber structure by increasing SA that decreasing the fiber storage modulus parameter.
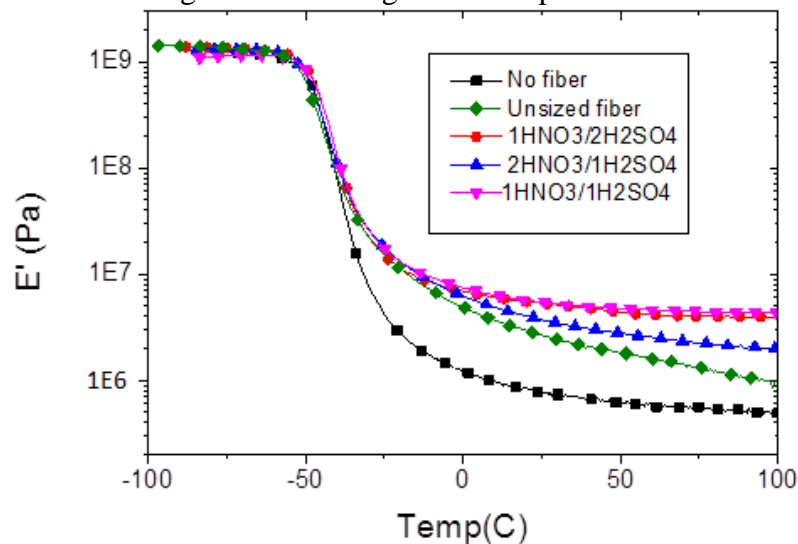

Fig. 7. The storage modulus of PU-CF composites as a function of temperature and surface treatment of fibers

By increasing polymer matrix/carbon fiber interaction, the modulus reduction value in the glass transition region decreased this subject confirms the carbon fiber reinforcement effect in the composite sample. According to Eq. 3, the ratio of modulus reduction in the composites

compared to pure resin is characterized by the C parameter [34]. The values of C parameters are shown in Table 3.

$$C = \frac{\left(E'_g/E'_r\right)_{composite}}{\left(E'_g/E'_r\right)_{resin}}$$

(3)

In Eq. 3, E'_g and E''_r indicate the storage modulus in glassy and rubbery regions, respectively. When the interaction between fiber and matrix is strong, the C parameter value is low. As shown in samples without any fibers, decreasing of storage modulus is high because in these samples the modulus in the rubbery region is controlled with amorphous chains. Due to the high resilience of the polymer chains and the low strength of the chains, the higher values of storage modulus decreasing is observed. The modulus in the glassy region is determined by intermolecular strength and the arrangement of the polymer chains together. In sample 1:1, the lowest value of this parameter is observed that confirming the strong intermolecular interaction between carbon fiber and PU matrix [35].

Table 3. The values of the C parameter for tested samples

Sample	C
Pure sample	1.00
Containing the unmodified fiber	0.58
1:2 (the ratio of NA to SA) containing the modified fiber	0.25
containing the modified fiber 1:1	0.10
containing the modified fiber 2:1	0.14

Loss coefficient (tanδ)

This parameter as a function of temperature is observed in Fig. 8. The characteristics of the loss parameter of materials have established the equilibrium between viscous and elastic phases. In composites, the mixing quality, kind, fiber distribution, fiber/matrix interaction, and free volume affect on loss parameter. All of the materials have the relaxation process that this property shows itself in the transition region from a glassy to rubbery state [35, 38].

The researchers showed the loss coefficient reaches the maximum value in the transition temperature but in the rubbery region, this parameter decreases. The relaxation process called α relaxation contains the movement of chains between the entanglements freely [38]. In the lower temperatures than Tg the loss parameter has a lower value because, in this region, the chains lie in a frozen state. Whereas in the transition region the chains start to move, and in this situation, the excess energy is released as thermal energy. Also in the rubbery region, there is a lower resistance against the chain movement, therefore in this region, the value of dissipation is low.

The location and the height of the tan ($δ$) peak indicate the structure and properties of composite material [39]. As a result, the loss value in composites is lower than in pure resin. Because in the composite samples most of the load is borne by the fiber, consequently the lower value of this load remains for the interfacial deformation, and dissipation of a strong interface is low. The other reason is the reduction of connected chains' movement to the fiber surface [40]. As shown in Fig. 8, in samples containing the modified carbon fiber, the height of the tan ($δ$) peak decreases showing the improvement of the interaction between carbon fiber and matrix due to fiber surface treatment. Also is observed that the Tg temperature with the addition of carbon fiber to the PU matrix decreases completely. The cause of this phenomenon is related to the weakness of the formation of a strong bond between the matrix and surface of carbon fiber.

In the pure matrix, the presence of the crosslink networks causes to decrease in chains movement capacity, whereas after the addition of carbon fibers (especially unmodified fiber) in the interfacial of PU/carbon fiber lie the chains containing the freely heads that they are not entered into the crosslink networks. This behavior causes to increase in the chain's mobility and

a decrease in Tg temperature. When there is a strong interaction between carbon fiber and PU matrix, the Tg parameter is encountered to lower decrease. As shown in Fig. 8, the addition of unmodified carbon fiber causes to decrease of 7 degrees of Tg temp from 237k to 230k, but in the case of the modified carbon fiber, this value is equal to 233k in the samples 1:2 and 2:1, whereas in sample 1:1 the Tg temp is 236k that this value shows the maximum amount of reinforcement effect in this sample.
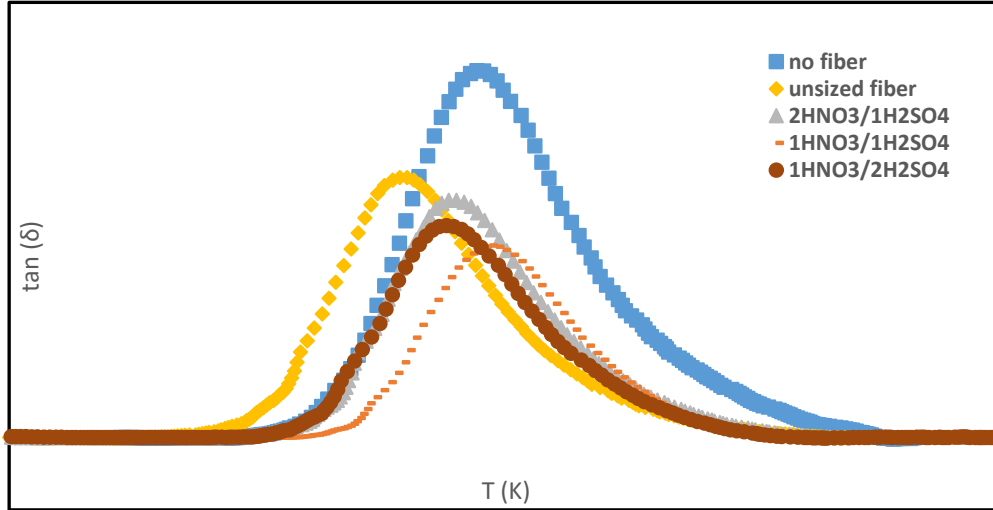

Fig. 8. The changes of tanδ against the temperature

Despite the suggested interpretations of the row data of dynamic and mechanical thermal analysis such as Tg, storage modulus, loss modulus, and the height of tan $δ$, the exact interpretation of composite behavior by investigating the sample figures is feasible [40]. The suitable method for this kind of investigation is applying the predictive models. For this purpose, the power low model was used. The power low model that is defined with Eq. 4 is an unsymmetrical function that both of its sides put on a baseline. Consequently, before matching the model on empirical data considering a suitable line both sides of the peak are put in the same direction.

$$\tan \delta = \frac{A}{[\omega \tau_0 (1 - T_0/T)^{-\alpha}]^{-m} + [\omega \tau_0 (1 - T_0/T)^{-\alpha}]^{-n}} \tag{4}$$

where τ_0 is relaxation time, ω is frequency, T_0 is transition temp, and m and n are the slopes of low and high-frequency curves. α parameter is defined as $\alpha = zv$ that v is critical power of correlation length and z is dynamic power [40]. The matching of the model on empirical data was carried out by the method of minimum errors of squared summation. In Fig. 9, the results of the matching model on empirical data are shown. The characterized variables were shown in the model in Table 4 and Fig. 10. Theα parameter is considered as a coefficient for matching the model and can be considered constant for the sampling of the process. In addition, the τ_0^{-1} coefficient has a frequency nature but considering molecular movement frequency, this parameter does not have any physical concept. Therefore α, m, and n parameters are compared with each other.
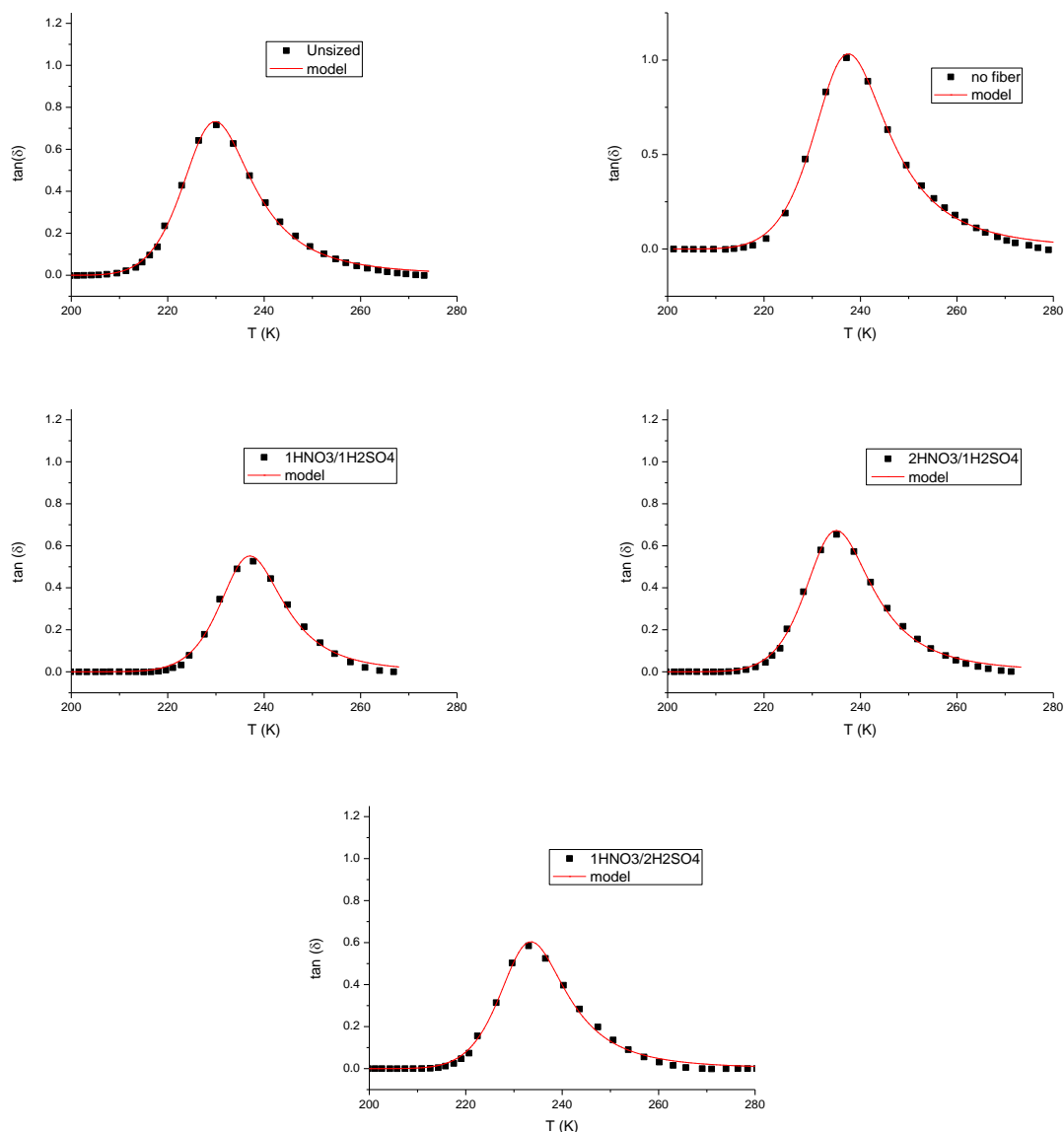
Fig. 9. Matching of the model to the empirical data. (a)Pure sample. (b) The sample contains unmodified carbon fiber. (c) The sample containing the modified carbon fiber 1:2 ((the ratio of NA to SA). (d) The sample containing the modified carbon fiber 1:1. (e) The sample containing the modified carbon fiber 2:1

Table 4. The matching of the power-low model parameters on the DMTA data

Sample	A	$_0\tau$	α	m	n
Pure sample	2.065727	0.0579	1.660022	2.344752	5.643687
the sample containing the unmodified carbon fiber	1.460939	0.040587	1.708919	2.445817	5.001052
the sample containing the modified carbon fiber 1:2((the ratio of NA to SA)	1.346428	0.007416	2.770987	4.807268	4.85376
the sample containing the modified carbon fiber 1:1	1.102871	0.178986	1.023232	8.783347	5.36606
the sample containing the modified carbon fiber 2:1	1.2074	0.01194	2.500744	3.874341	4.137412

As shown *A* and *n* don't show any changes, whereas in the samples containing the carbon fiber *m* parameter increases compared to pure resin. The m coefficient is similar to the *h* coefficient in the Cole-Cole model (According to Eq. 5 and Fig. 11), and it is related to chains that have a long relaxation time. The increase of the *h* parameter indicates the enhancement of

interaction between modified fibers and resin. Also, it can be observed that modification of fibers can increase the h parameter. The results show that the maximum amount of *h* is in sample 1:1. This phenomenon shows enough value of acid for the formation of carboxyl groups and on the other hand, this value doesn't have any degradable effect on the inherent properties of carbon fiber. In addition, the investigation of changes in the intrachain crosslinks is carried out with a drawing of complex modulus in complex coordination that is called as Cole-Cole model.
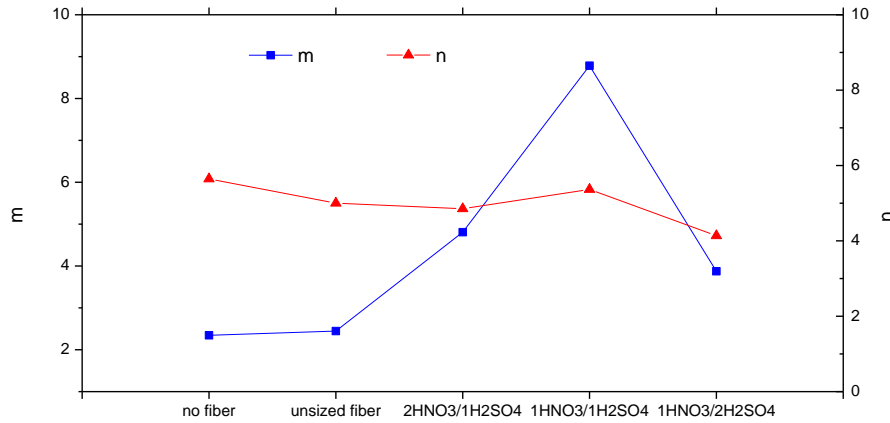

Fig. 10. m,n parameters obtained from power low model

On the other hand, this value does not have any degradable effect on the inherent properties of carbon fiber. In addition, the investigation of changes in the intrachain crosslink is carried out with a drawing of complex modulus in complex coordination called as Cole-Cole model.

$$E^* = E_0 + \frac{E_\infty - E_0}{1 + (i\tau_1)^{-h} + (i\tau_2)^{-k}} \qquad (5)$$

In Eq. 5, τ_1 and τ_2 are relaxation times, and the *h*, *k* parameters are related to high temperature (long time) and low temperature (short time), respectively. E_0 and E_∞ are relaxing modulus and unrelaxed modulus, respectively, observed in Fig. 11. In addition, about other samples, the amount of these parameters are shown in Table 5 that these results are matched with obtained results of low power model on the tanδ results. In these results increasing of h parameter indicates the positive effect of carbon modification on the interaction between resin and carbon fibers.
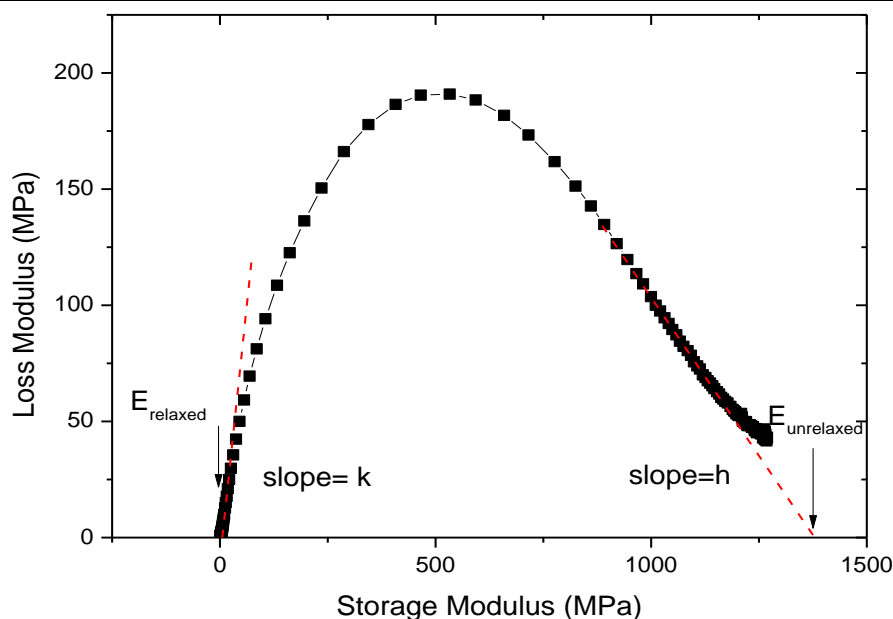
Fig. 11. The cole-cole curve of pure resin

Table 5. The h, k parameters obtained from the cole-cole curve

Sample	h	K
Pure sample	0.2421	1.1405
Sample containing the unmodified carbon fiber	0.3519	0.7938
Sample containing the modified carbon fiber 1:1	0.4195	0.7264
Sample containing the modified carbon fiber 1:2((the ratio of NA to SA)	0.3631	0.6428
Sample containing the modified carbon fiber 2:1((the ratio of NA to SA)	0.4003	0.6273

Conclusion

In this work, the effect of carbon fiber oxidation in the different rations of NA to SA on the carbon fiber modification and interaction between fiber and Polyurethane matrix was investigated. The FTIR results showed the formation of carbonyl groups in the low power of oxidation, carboxyl groups in the high power of oxidation, and the shift of the C=O peak toward lower wavenumbers. These results associated with new peaks contributed to N-H and NCO confirm the covalent reaction between modified carbon fiber and finish agent. The XRD results showed the presence of functional groups and degradation of carbon crystal sheets. The SEM images showed the effect of acid oxidation on the carbon fiber surface. The interaction between carbon fiber and PU matrix was investigated by DMTA analysis. In all samples, increasing in elastic modulus due to the addition of carbon fiber to the PU matrix was observed. In addition, the modulus increase in the samples containing the modified carbon fiber was more than in samples containing the unmodified carbon fiber. According to decreasing trend of carbon fiber modulus lonely, increasing of final PU modulus can indicate the good effect of fiber modification on the improving interaction between carbon fiber and PU resin. Whereas this increasing process was not linear and in the oxidized sample with a solution containing the strong acidity property, the presence of the more functional groups compared to sample 1:1 was observed lower modulus. The tanδ diagrams showed the decreasing glass transition in all of the samples containing the carbon fibers compared to the pure resin that this issue is related to the weak interaction between carbon fiber and PU matrix. As shown the decrease of *Tg* temp with increasing of carbon fiber/PU interaction had a low intensity. In addition, the matching results of the power-low model and Cole-Cole diagram on the DMTA results showed the increasing

of chains with the long relaxation time following the carbon fiber modification that confirming the strong interaction in these samples.

Nomenclature

C	Modulus ratio (-)
E'_g	Storage modulus in the glassy region (MPa)
E'_r	Storage modulus in the rubbery region (MPa)
$\tan\delta$	Loss coefficient (-)
Tg	Glass transition temp (k)
τ_0	Relaxation time (sec)
ω	Frequency (Hz)
T_0	Transition temp (k)
m	The slope of low-frequency curves (-)
n	The slope of high-frequency curves (-)
v	The critical power of correlation length (-)
z	Dynamic power, dimensionless
τ_1	Relaxation time1 (sec)
τ_2	Relaxation time2 (sec)
h	Related Parameter to high temperature (long time) (-)
k	Related Parameter to low temperature (short time) (-)
E_0	Relax modulus (MPa)
E_∞	Un-relax modulus (MPa)

References

[1] Frenzel H, Mäder E. Influence of different interphases on the mechanical properties of fiber-reinforced polymers, in Interfaces, Surfactants and Colloids in Engineering. H.J. Jacobasch. 1996:199-202.

[2] Sánchez A M .Influence of the nature and the content of carbon fiber on properties of thermoplastic polyurethane-carbon fiber composites. Journal of applied polymer science. 2003; 90:2676-2683.

[3] Zo H J. Enhanced mechanical and thermal properties of carbon fiber composites with polyamide and thermoplastic polyurethane blends. Fibers and Polymers. 2014; 15:1071-1077.

[4] Husić S, Javni I, Petrović Z S.Thermal and mechanical properties of glass reinforced soy-based polyurethanecomposites. Composites Science and Technology. 2005; 65: 19-25.

[5] Lu X. Moisture–absorption, dielectric relaxation, and thermal conductivity studies of polymer composites. Journal of Polymer Science Part B: Polymer Physics, 1998; 36: 2259-2265.

[6] Chou P J, Ding D. Characterization of moisture absorption and its influence on composite structures. Journal of Thermoplastic Composite Materials. 2000; 13: 207-225.

[7] Corrêa R A, Nunes R C, Lourenço V L. Investigation of the degradation of thermoplastic polyurethane reinforced with short fibres. Polymer degradation and stability. 1996; 52: 245-251.

[8] Chen C H, Ma C C M. Pultruded fiber reinforced blocked polyurethane (PU) composites. I. Processability and mechanical properties. Journal of applied polymer science. 1992; 46: 937-947.

[9] Hou L L, Liu H Z, Yang G S. A novel approach to the preparation of thermoplastic polyurethane elastomer and polyamide 6 blends by in situ anionic ring-opening polymerization of ε-caprolactam. Polymer international. 2006; 55: 643-649.

[10]   Zang Z. Mechanical property improvement of plasma treated carbon fiber-reinforced polyurethanes (PUR) composites with SiO2 filler. Polymer-Plastics Technologyand Engineering. 2012; 51: 696-700.

[11]   Zhang Z Z. Effect of carbon fibers surface treatment on tribological performance of polyurethane (PU) composite coating. Wear. 2008; 264: 599-605.

[12]   Tiwari S. Influence of cold remote nitrogen oxygen plasma treatment on carbon fabric and its composites with specialty polymers. Journal of Materials Science. 2011; 46: 964-974.

[13]   Baun W. Anodization of evaporated aluminium on Ti-6 wt% Al-4 wt% V. Journal of Materials Science. 1980; 15: 2749-2753.

[14]   Wilson W, Haggmark L, Biersack J. Calculations of nuclear stopping, ranges, and straggling in the low-energy region. Physical Review B. 1977; 15: 2458.

[15]   Wan Y. Effect of surface treatment of carbon fibers with gamma-ray radiation on mechanical performance of their composites. Journal of materials science. 2005; 40: 3355-3359.

[16]   Li J. High-energy radiation technique treat on the surface of carbon fiber. Materials Chemistry andPhysics. 2005; 94: 315-321.

[17]   Tang L G. Kardos J L. A review of methods for improving the interfacial adhesion between carbon fiber and polymer matrix. Polymer composites. 1997; 18: 100-113.

[18]   Sellitti C, Koenig J, Ishida H. Surface characterization of graphitized carbon fibers by attenuated total reflection Fourier transform infrared spectroscopy. Carbon. 1990; 28: 221-228.

[19]   Chen S, Feng J. Epoxy laminated composites reinforced with polyethyleneimine functionalized carbon fiber fabric: Mechanical and thermal properties. Composites Science and Technology. 2014; 101: 145-151.

[20]   Tran M Q. Carbon fibre reinforced poly (vinylidene fluoride): impact of matrix modification on fibre/polymer adhesion. Composites Science and Technology. 2008; 68: 1766-1776.

[21]   Rand B, Robinson R. Surface characteristics of carbon fibres from PAN. Carbon. 1977; 15: 257-263.

[22]   Jang J, Yang H. The effect of surface treatment on the performance improvement of carbon fiber/polybenzoxazine composites. Journal of materials science. 2000; 35: 2297-2303.

[23]   Zhang X. Effects of carbon fiber surface treatment on the tribological properties of 2D woven carbon fabric/polyimide composites. Applied Physics A. 2009; 95: 793-799.

[24]   Li J. The effect of surface modification with NA on the mechanical and tribological properties of carbon fiber-reinforced thermoplastic polyimide composite. Surface and Interface Analysis. 2009; 41: 759-763.

[25]   Zhang X .Pei X, Wang Q. The effect of fiber oxidation on the friction and wear behaviors of short-cut carbon fiber/polyimide composites. Expr. Polym. Lett. 2007; 1: 318-325.

[26]   Su F h. Tribological and mechanical properties of the composites made of carbon fabrics modified with various methods. Composites Part A: Applied Science and Manufacturing. 2005; 36: 1601-1607.

[27]   Tiwari S, Bijwe J, Panier S. Tribological studies on polyetherimide composites based on carbon fabric with optimized oxidation treatment. Wear. 2011; 271: 2252-2260.

[28]   Park S J, Park B J. Electrochemically modified PAN carbon fibers and interfacial adhesion in epoxy-resin composites. Journal of materials science letters. 1999; 18: 47-49.

[29]   Xu Z. Graphitization of polyacrylonitrile carbon fibers and graphite irradiated by γ rays. Materials Letters. 2009; 63: 1814-1816.

[30]   Lim S. Surface modification of carbon nanofiber with high degree of graphitization. The Journal of Physical Chemistry B. 2004; 108:1533-1536.

[31]   Gupta A, Harrison I R., Lahijani J. Small-angle X-ray scattering in carbon fibers. Journal of applied crystallography. 1994; 27: 627-636.

[32]   Meneghetti P, Qutubuddin S. Synthesis, thermal properties and applications of polymer-clay nanocomposites. Thermochimica Acta. 2006; 442: 74-77.

[33]   Ramanathan T. Functionalized graphene sheets for polymer nanocomposites. Nature nanotechnology. 2008; 3: 327-331.

[34]   Pothan L A, Oommen Z, Thomas S. Dynamic mechanical analysis of banana fiber reinforced polyester composites. Composites Science and Technology. 2003; 63: 283-293.

[35]   Martin O, Averous L. Poly (lactic acid): plasticization andproperties of biodegradable multiphase systems. Polymer. 2001; 42: 6209-6219.

[36] Amash A, Zugenmaier P. Thermal and dynamic mechanical investigations on fiber-reinforced polypropylene composites. Journal of Applied Polymer Science. 1997; 63: 1143-1154.

[37] Fornes T, Paul D. Modeling properties of nylon 6/clay nanocomposites using composite theories. Polymer. 2003; 44: 4993-5013.

[38] Randrianantoandro H. Viscoelastic relaxation of polyurethane at different stagesof the gel formation. 1. Glass transition dynamics. Macromolecules. 1997; 30: 5893-5896.

[39] Ornaghi H L. Mechanical and dynamic mechanical analysis of hybrid composites molded by resin transfer molding. Journal of Applied Polymer Science. 2010; 118: 887-896.

[40] Harris B. Study of carbon fibre surface treatments by dynamic mechanical analysis. Journal of materials science. 1993; 28: 3353-3366 .

[41] Florek P, Król M, Jele P, Mozgawa W. Carbon Fiber Reinforced Polymer Composites Doped with Graphene Oxide in Light of Spectroscopic Studies. Materials. 2021; 14: 1835.

[42] Hwang D , Lee S G, Cho D. Dual-Sizing Effects of Carbon Fiber on the Thermal, Mechanical, and Impact Properties of Carbon Fiber/ABS Composites. Polymers; 2021, 13: 2298.

[43] Zhao D, Hamada H, Yang Y. Influence of polyurethane dispersion as surface treatment on mechanical, thermal and dynamic mechanical properties of laminated woven carbon-fiber-reinforced polyamide 6 composites. Composites Part B. 2019; 12:105